Helical Molecular Programming: Folding of Oligopyridine-dicarboxamides into Molecular Single Helices

Volker Berl,[a, b] Ivan Huc,*[c] Richard G. Khoury,[a] and Jean-Marie Lehn*[a]

Abstract: Molecular strands composed of alternating 2,6-diaminopyridine and 2,6-pyridinedicarbonyl units have been designed to self-organize into single stranded helical structures upon forming intramolecular hydrogen bonds. Pentameric strands **11**, **12**, and **14**, heptameric strands **1** and **20**, and undecameric strand **15** have been synthesized using stepwise convergent strategies. Single helical conformations have been characterized in the solid state by single crystal X-ray diffraction analysis for four of these compounds. Helices from pentameric strands **12** and **14** extend over one turn, and helices from heptameric **20** and undecameric **15** species extend to one and a half and two and a half turns, respectively. Intramolecular hydrogen bonds are responsible for the strong bending of the strands. ^{1}H NMR shifts both in polar and nonpolar organic solvents indicate intramolecular overlap between the peripheral aromatic groups. Thus, helical conformations also predominate in solution. Molecular stochastic dynamic simulations of strand folding starting from a high energy extended linear conformer show a rapid (600 ps at 300 K) conversion into a stable helical conformation.

Keywords: helical structures · conformation analysis · folding · hydrogen bonds · self-assembly

Introduction

The biological functions of biopolymers such as nucleic acids and proteins rest on their folding into three-dimensional architectures which involve a complex interplay of numerous intramolecular nonbonding interactions. Recently, interest has grown for artificial oligomers and polymers also undergoing self-organization into well-defined conformations. These compounds provide simple models in which the thermodynamic and kinetic parameters of folding are more easily assessed than in biopolymers. They may also be used as frameworks to elaborate not only structural but also functional mimics of biological compounds.

Among the structural patterns encountered in biopolymers, single helical conformations have been the focus of special attention, leading to their implementation in numerous synthetic systems.[1] A majority of these operate through intramolecular attractive and/or repulsive interactions to restrict conformations and induce bending of molecular strands into helices. Thus, as in natural peptides, intramolecular hydrogen bonding in synthetic aromatic[2] and aliphatic[3] oligoamides leads to helical winding of the strand. Preferential conformations within extended pyridine – pyrimidine,[4] pyridine – pyridazine,[5] or pyridine – pyrazine[6] sequences result in well-defined helical conformations. In such polyaromatic compounds, stacking between aromatic residues within the helical structure provides an additional driving force for helical folding.[2, 4–7] Single helical molecular shapes may be enforced through covalent conformational restriction. In this case, the molecules are completely preorganized in a helix, and their unfolding would require covalent bond breaking.[8, 9] More or less flexible molecular strands may also organize in single helices upon coordinating to metal ions[10] or as a result of solvophobic effects.[11] Finally, supramolecular single helices can be generated by self-assembly of small molecules in the solid or in solution.[12]

We recently reported on a new family of oligomeric molecular strands based on pyridine carboxamides.[13a] Intramolecular hydrogen bonds lead to the folding of these structures into single helical conformers, which assemble to form double helical dimers. Herein, we give an extensive description of the design principles, synthesis, and initial folding of these oligomers into single helices in solution and in the solid.

[a] Prof. Dr. J.-M. Lehn, Dr. V. Berl, Dr. R. G. Khoury
Laboratoire de Chimie Supramoléculaire
ESA 7006 of the CNRS, ISIS, Université Louis Pasteur
4 rue Blaise Pascal, 67000 Strasbourg (France)
Fax: (+33) 388 411020
E-mail: lehn@chimie.u-strasbg.fr

[b] Dr. V. Berl
Affiliated institution: Forschungszentrum Karlsruhe GmbH
Institut für Nanotechnologie, Postfach 3640
76021 Karlsruhe (Germany)

[c] Dr. I. Huc
Institut Européen de Chimie et Biologie, ENSCPB
Av. Pey Berland, 33402 Talence Cedex (France)
Fax: (+33) 557 962226
E-mail: ivan.huc@iecb-polytechnique.u-bordeaux.fr

  0947-6539/01/0713-2798 $ 17.50+.50/0

Results and Discussion

Design of the components: Molecular strands such as **1** are oligomers composed of alternating 2,6-diaminopyridine and 2,6-pyridinedicarbonyl units (Figure 1).[13a] They were designed as pyridine analogues of the oligoisophthalamide **2** described earlier.[14] In all these compounds, conformational preferences at the pyridine–NH and CO–NH linkages restrict rotations about these bonds: The amide bond prefers a *trans* conformation; the carbonyls establish favorable contacts with aromatic protons in position 3 or 5 of the diaminopyridine rings; and the $N^{\delta-}H^{\delta+}$ dipoles are antiparallel to the neighboring pyridine nitrogen lone pairs. This sets the pyridinaminocarbonyl moiety in an overall planar geometry.

In the oligoisophthalamide series, the rotation about the CO–aryl bonds has a low energy barrier, and leads to multiple different quasiplanar/conjugated rotamers. Upon hydrogen bonding of the diamino-pyridine units to a complementary cyanurate template, curvature is introduced in the backbone. Within heptamer **2**, binding of two template molecules stabilize three rotamers of C, S and helical shape (Figure 1).[14]

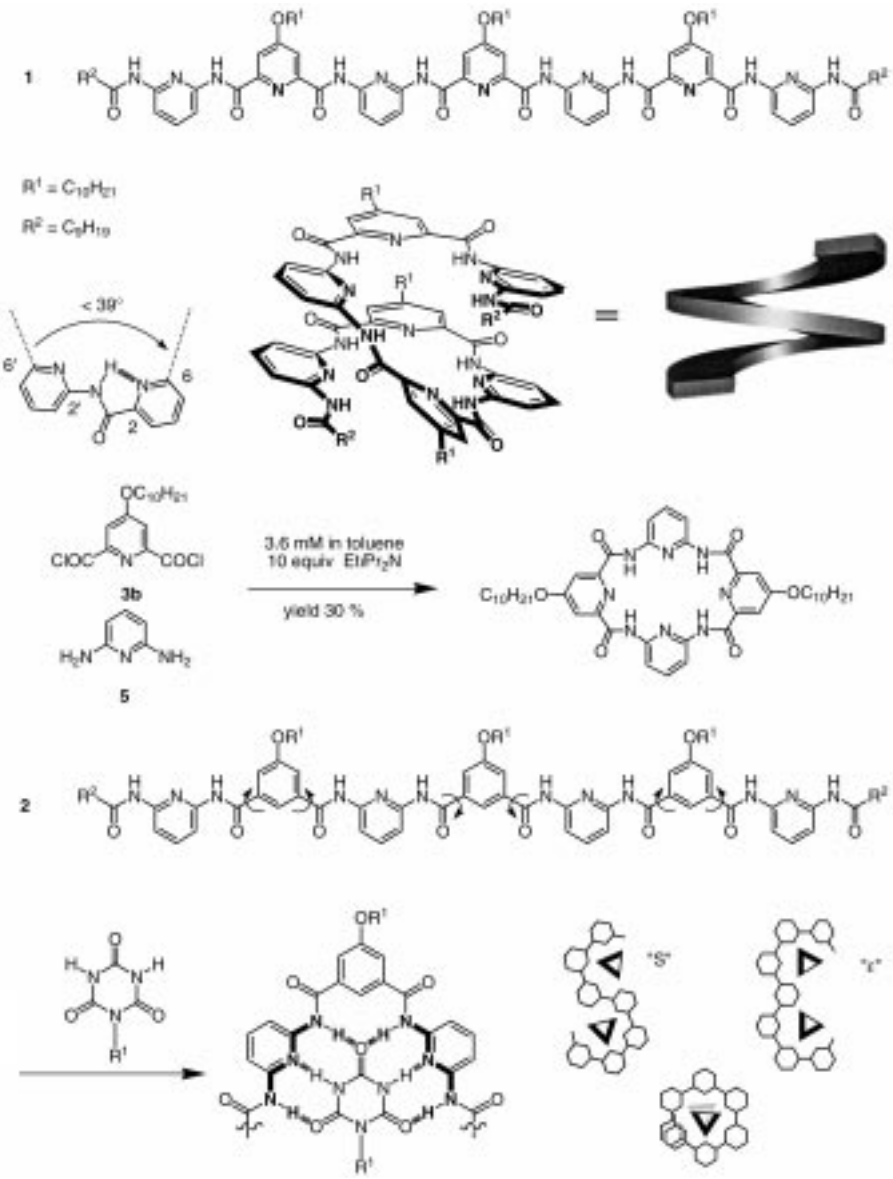

Figure 1. Structure of molecular heptameric strands **1** and **2**. Intramolecular hydrogen bonds lead to the folding of **1** into a molecular single helix (top). They may also play a role in the formation of a tetrameric macrocycle from 2,6-diaminopyridine and 4-decyloxy-2,6-pyridine dicarbonyl chloride (middle). Binding of two template cyanurate molecules to **2** leads to the stabilization of three conformers of "S", "ε", and helical shape (bottom).

In the pyridine 2,6-dicarboxamide series, the nitrogen atoms introduced are expected to hydrogen bond to the neighboring amide hydrogens. These intramolecular hydrogen bonds should direct rotations about the CO–aryl linkages towards a bent conformation and favor a helical shape of the molecule in the absence of any template. Modeling studies of the 2-pyridyl–2-pyridinecarboxamide helical codon (MacroModel, Amber force field)[15] suggest that, in the bent hydrogen-bonded conformation, substituents at the 6 and 6′ positions define an angle of about 39°. Crystallographic data on analogous structures available from the Cambridge

Abstract in French: *Des brins moléculaires constitués d'unités alternantes 2,6-diaminopyridine et 2,6-pyridinedicarbonyle ont été conçus dans le but d'induire une auto-organisation en structures hélicoïdales par formation de liaisons hydrogène intramoléculaires. Des brins pentamériques **11**, **12** et **14**, heptamériques **1** et **20** et undécamérique **15** ont été synthétisés par étapes selon une stratégie convergente. Les conformations en simple hélice ont été caractérisées à l'état solide par diffraction des rayons X pour quatre de ces composés. Les brins pentamériques **12** et **14**, heptamérique **20** et undécamérique **15** forment des hélices à un tour, 1.5 tours et 2.5 tours, respectivement. La forte courbure des brins est imposée par des liaisons hydrogène intramoléculaires. Les déplacements chimiques des signaux de RMN ^{1}H indiquent un recouvrement intramoléculaire entre les groupes aromatiques périphériques, confirmant la prédominance des conformations hélicoïdales en solution. Des simulations stochastiques par dynamique moléculaire du repliement d'un brin à partir d'un conformère linéaire d'énergie élevée montrent une conversion rapide (600 ps à 300 K) en une conformation hélicoïdale stable.*

Crystallographic Database (CCDC) confirm this prediction with values as low as 35°,[16] which are noticeably smaller than the 60° expected for sp^2 centers with a planar trigonal 120° symmetry.

This preferred conformation may play a role in the formation of a tetrapyridyl macrocycle from the condensation of 2,6-diaminopyridine (**5**) and 4-decyloxy-pyridine-2,6-dicarbonyl dichloride (**3b**) (Figure 1), in 30% yield in relatively concentrated conditions (3.6 mM), pointing to a predisposition of the system towards cyclization. Moreover, no larger cycles were detected, including the cyclic hexamer expected for sp^2 centers with a planar trigonal 120° symmetry.[17]

As a consequence of this strong bent, a helical motif (i.e., the overlap of the strand extremities) should emerge for strands containing as few as five aromatic rings. Heptamer **1** is expected to undergo nearly one and a half turns. In the helical form, substituents in position 4 of the pyridine rings protrude radially and may enhance the solubility of these compounds in aromatic and chlorinated solvents.

Synthesis: Two distinct strategies were developed for the preparation of oligopyridine-dicarboxamides having an odd number of aromatic rings. At first, a route derived from the synthetic Scheme of oligoisophthalamide **2** was followed.[14] It was initially designed so as to converge in only three key steps to a heptamer composed of four 2,6-diaminopyridine and three 2,6-pyridinedicarbonyl units. The first step involved the double condensation of a 2,6-diaminopyridine monolithium salt to a pyridine-2,6-dicarboxylic acid dimethyl ester to give in low but acceptable yield a trimer possessing two amine functions (Schemes 1 and 2). One of these two amines was subsequently acylated with acetyl chloride or decanoyl chloride. And the resulting monoamine was exposed to half an equivalent of a pyridine-2,6-dicarbonyl dichloride to yield the corresponding heptamer.

Heptamer **1** which has solubilizing decyloxy chains in position four of the pyridine rings and decanoyl end-capping residues was synthesized according to this Scheme (Scheme 1). Prior to this, the starting 4-decyloxy-pyridine-2,6-dicarboxylic acid dimethyl ester (**4**) was prepared from chelidamic acid using standard procedures. Pyridinedicarboxylic acid (**3**) was prepared in two steps upon treatment of chelidamic acid with decanol in H_2SO_4 followed by saponification of the decyloxyester functions. It was then converted to the corresponding diacid chloride, and dimethyl ester **4**. As expected, the alkoxy substituents provide **1** with a high solubility in chlorinated and aromatic solvents. This substance, however, is not prone to crystallization, which led us to consider analogous compounds lacking the alkoxy chains.

When the same Scheme was applied to commercially available 2,6-diaminopyridine (**5**) and pyridine-2,6-dicarboxylic acid dimethyl ester (**9**), the initial condensation step in the presence of an excess of the monolithium salt of **5** yielded the expected diamine trimer **10**, but the unexpected diamine pentamer **11** was also isolated (Scheme 2). Trimer **10** has very low solubility in most common organic solvents, which hampered its conversion to the corresponding heptamer. Monoacylation conditions (one equivalent of acyl chloride) applied to suspension of **10** in THF, for example, yielded quantitatively the bis-acylated product. After the first heterogeneous acylation, the monoacylated product is solubilized and readily acylated a second time in solution.

On the other hand, the diamine pentamer **11** is remarkably more soluble than trimer **10** and proved to be a suitable material for further functionalization, giving access to various pentamers and to the undecamer **15**. It could be diacylated with acetyl chloride to pentamer **12**. Fmoc mono-protection in THF led to the desired mono-protected **13** and to the bis-protected **14** as a side product. Upon exposure to half an equivalent of pyridine-2,6-dicarbonyl dichloride, immediately followed by a deprotection step using piperidine in DMF, compound **13** was converted to the diamine undecamer **15** (Scheme 2). Diamine **15** could only be dissolved in hot DMSO, which precluded any further transformation.

This approach thus provided pentamers, heptamers and an undecamer in a highly convergent fashion. It cannot, however, be applied to the synthesis of longer chains because of the irreversible acylation of the terminal amino groups (in the case of **1**), or because of the insolubility of the final product (in

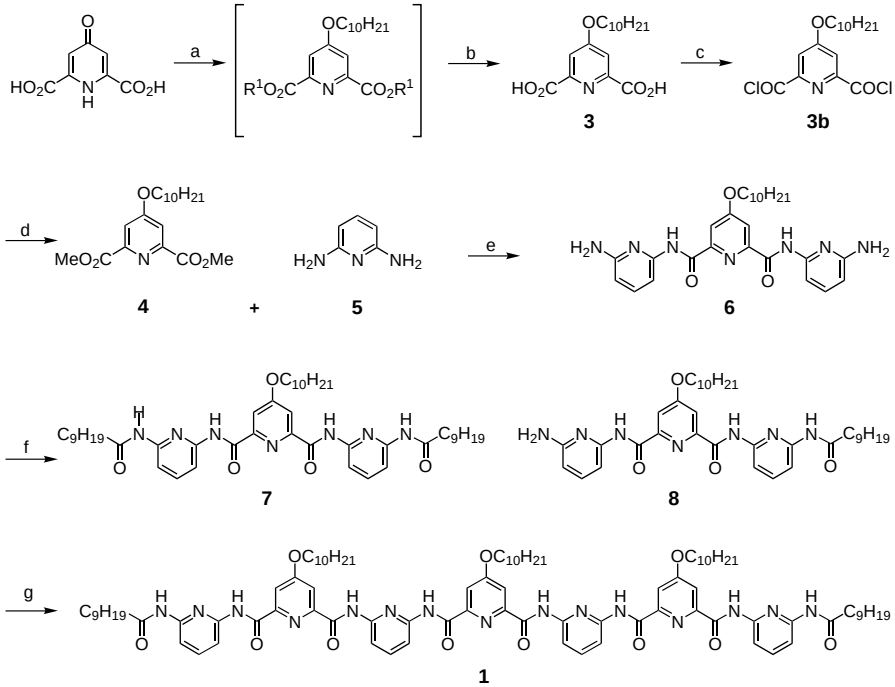

Scheme 1. Synthesis of **1**: a) decanol, H_2SO_4, toluene, Dean–Stark, reflux; b) KOH/EtOH, reflux; c) $SOCl_2$, reflux; d) MeOH, 0 °C; e) *n*BuLi, THF, −78 °C; f) $C_9H_{19}COCl$, NEt_3, THF, 0 °C; g) **3b**, NEt_3, THF, 0 °C.

0947-6539/01/0713-2800 $ 17.50+.50/0 *Chem. Eur. J.* **2001**, *7*, No. 13

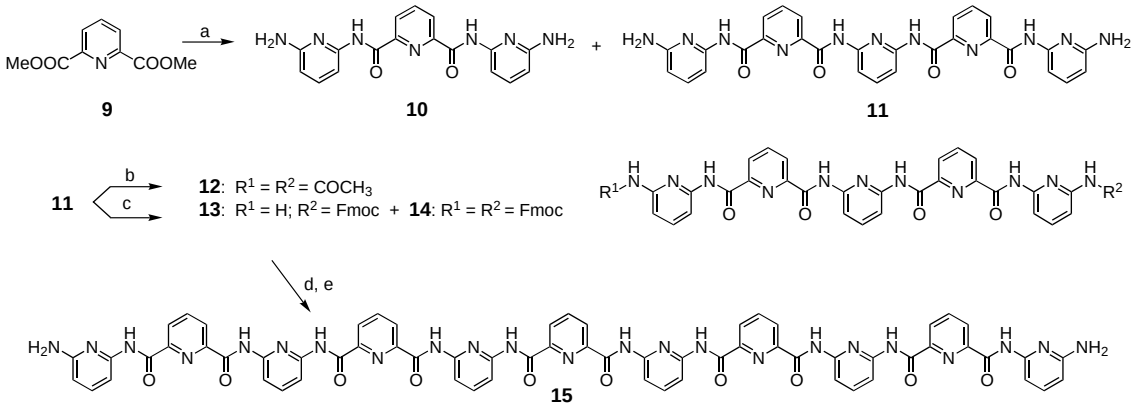

Scheme 2. Synthesis of **15**: a) **5**, *n*BuLi, THF, $-78\,^{\circ}C$; b) CH_3COCl, NEt_3, THF, r.t.; c) FmocCl, NEt_3, THF, r.t.; d) 2,6-pyridinedicarbonyl dichloride, NEt_3, THF, r.t.; e) piperidine, DMF.

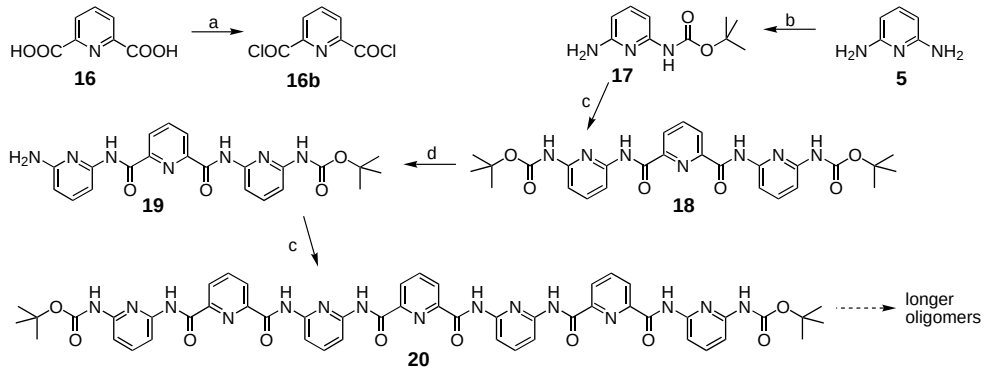

Scheme 3. Synthesis of **20**: a) $SOCl_2$, reflux; b) LiHMDS, Boc_2O, THF, r.t.; c) **16b**, NEt_3, THF, r.t.; d) TMSI, chloroform, then MeOH, reflux.

the case of **15**). With the intent to develop a more versatile and divergent strategy that could be applied iteratively to build oligomers of increasing length, we explored the possibility of effecting mono-deprotections on oligomers bearing two terminal Boc-protected amino residues.

As shown in Scheme 3, 2,6-diaminopyridine (**5**) was efficiently monoprotected after treatment with LiHMDS, followed by Boc-anhydride. The monoamine **17** obtained reacted with pyridine-2,6-dicarbonyl dichloride to afford the corresponding bis-Boc-protected trimer **18**. Upon exposure of this compound to a stoichiometric amount of TMSI, followed by hydrolysis in methanol, the monoamine **19** was obtained in 61 % yield. This amine was subsequently coupled to pyridine-2,6-dicarbonyl dichloride to yield bis-Boc-protected heptamer **20**. Despite the lack of alkoxy chains, **20** is soluble in chlorinated solvents, perhaps because helical wrapping (see below) hinders intermolecular association; the same may hold for **11**.

Thus, the mono-deprotection of a bis-Boc-protected diamine using TMSI followed by reaction with pyridine-2,6-dicarbonyl dichloride easily leads to a heptamer lacking alkoxy chains which could not be obtained otherwise for solubility reasons. If these two steps can be iterated, this strategy should give access to longer chains having $2^n - 1$ aromatic rings (15, 31, 63…). We are currently exploring this prospect.

Single helix formation in the solid state: For all the newly synthesized compounds, attempts were made to get single crystals suitable for X-ray diffraction. A number of solvent combinations and diffusion techniques were tested. Crystals from heptamer **1**, which bear decyloxy chains in position 4 of the pyridine rings, were difficult to obtain and were either too small, or disordered. On the other hand, compounds lacking long alkyl chains were highly crystalline. Thus, liquid/liquid diffusion setups yielded good quality single crystals of pentamers **12** and **14**, heptamer **20**,[13] and undecamer **15**, which could all be analyzed by X-ray diffraction. The crystal characteristics and crystallographic parameters are summarized in Table 1.

In the crystal, the four oligomeric strands adopt a single helix conformation closely matching the predicted structures (Figures 2a–c and 3). All pyridine–NH, NH–CO and CO–pyridine bonds present the expected conformation. Within pyridinecarboxamide groups, an intramolecular hydrogen bond forms between the amide NHs and the pyridine nitrogen. Typical amide N*H* pyridine–*N* distances are between 2.21 and 2.24 Å. Typical amide *N*H–pyridine *N* distances are between 2.65 and 2.74 Å. The bending of the oligomers is such that an overlap of the strand extremities leading to the helical motif is possible for pentamers **12** and **14** (Figure 2a, b). For compound **14**, the Fmoc aromatic groups at the strand extremities do not belong to the helical structure

Table 1. Crystallographic parameters for the structures determined.

Compound	**12**	**14**	**20** (single helix)	**15**
M_W	$C_{33}H_{27}N_{11}O_6 \cdot 2(CH_3OH) \cdot (H_2O)$	$C_{59}H_{43}N_{11}O_4 \cdot 0.25(CH_3OH) \cdot 1.5(CHCl_3) \cdot (H_2O)$	$C_{51}H_{47}N_{15}O_{10} \cdot 2(C_2H_6SO) \cdot 2(H_2O) \cdot 1.5(C_2H_3N)$	$C_{65}H_{47}N_{23}O_{10} \cdot 1.5(H_2O) \cdot 0.5(CH_3OH)$
crystallizing solvent/	DMSO/	chloroform/	DMSO/	DMSO/
precipitant	methanol	hexane	acetonitrile	methanol
crystal dimensions [mm]	$0.21 \times 0.15 \times 0.15$	$0.30 \times 0.25 \times 0.20$	$0.25 \times 0.16 \times 0.15$	$0.16 \times 0.08 \times 0.05$
color	colorless	colorless	colorless	colorless
unit cell	monoclinic	triclinic	monoclinic	monoclinic
space group	*C*2/*c*	$P\bar{1}$	*C*2/*c*	*C*2/*c*
dimensions				
a [Å]	16.250(3)	13.202(3)	33.952(7)	17.451(4)
b [Å]	24.110(5)	15.309(3)	13.510(3)	27.226(5)
c [Å]	18.070(4)	15.806(3)	27.97(6)	13.123(3)
angles				
α [°]	90	80.59(3)	90	90
β [°]	91.78(3)	87.87(3)	97.75(3)	102.59(3)
γ [°]	90	68.69(3)	90	90
V [Å^3]	7076(2)	2935(1)	12713(4)	6085(2)
Z	8	2	8	4
FW [g mol^{-1}]	755.75	1253.77	1283.91	1353.28
ρ [g cm^{-3}]	1.265	1.411	1.367	1.430
scanned θ	$2.02^\circ \le \theta \le 27.45^\circ$	$1.31^\circ \le \theta \le 27.48^\circ$	$1.0^\circ \le \theta \le 27.6^\circ$	$0.67^\circ \le \theta \le 8.60^\circ$
total/unique refl.	13544/3730	13315/6450	14359/7699	25540/4479
parameters	485	779	802	457
GOF	0.952	0.916	1.067	0.952
res. e$^-$ density [e Å^{-3}]	0.684	0.540	0.933	1.038
*R*1 [%]	**8.7**	**7.6**	**11.7**	**7.8**
CCDC Ref.	147333	147334	142810	147335

and are positioned perpendicular to the helix plane. The approximate value of 4.5 rings per helix turn leads to one and a half turn for heptamer **20** and nearly two and half turns for undecamer **15**.

Table 2 gives a comparative presentation of the four structures. In all cases, aromatic ring *n* overlaps with aromatic ring *n*+4. The helical pitch (e.g. the distance along the helix axis between ring *n* and ring *n*+4) is consistently around 3.6 Å. This indicates a tight contact between aromatic rings, suggesting that stacking likely plays a role in the cohesion of the structure. Owing to the alternation of diaminopyridine rings and pyridinedicarbonyl rings, intramolecular aromatic stacking occurs essentially within rings of the same nature.

The helices and voids of their cavity have an elliptical shape (see top views in Figure 2a, b). Typical values for the axes of a helix are 13.5 Å and 11.1 Å. The axes of the internal voids are 8.1 Å and 5.6 Å long, respectively. Most polar functions of the oligopyridine-dicarboxamides are converging towards the interior of the helices, where bound co-crystallized water molecules are seen in each case. Solvent molecules are also present in all structures (not shown in the Figures), but they are located between the helices and not in their interior.

The formation of a helix imposes a slight deviation from the preferred planar conformations of the molecular strand. The resulting torsional angles between consecutive aromatic rings is similar from structure to structure (13.4° on average), but it varies significantly within the same strand depending on whether the rings have central or terminal positions. Terminal rings are significantly less tilted than average for compounds **12**, **14**, and **20**. They are significantly more tilted for undecamer **15** (see below).

For a symmetrical helical structure, the line going through the nitrogen atom and C4 carbon atom of the central pyridine ring should be a C_2-symmetry axis. The helix formed by undecamer **15** is indeed perfectly C_2 symmetrical, and the line going through the nitrogen and C4 carbon atoms of the central pyridine ring is a crystallographic symmetry axis. Thus, the crystallographic asymmetric unit cell only contains half a helix. On the other hand, the helices formed by **12**, **14**, and **20** deviate slightly from a perfect C_2 symmetry. As shown in Table 2, the series of torsional angles between consecutive pyridine rings at the two strand termini are not identical. As a result, the crystallographic unit cell contains an entire strand. All four structures belong to a nonchiral space group, which means that plane symmetrical right- and left-handed helical strands are present in the crystal.

The folding pattern of the four structures is overall highly conserved, leading to structurally similar helices. However, a

Table 2. Characteristics of the helical structures in the solid.

Compound	Helical pitch torsional angles [°]	Pyridine–pyridine of the elipsoidal objects [Å]	Outer diameters of elipsoidal cavity [Å] C–C atom center distances	Inner diameters mode[b] N–CN atom center distances	Overlapping
12	3.59[a]	7.7, 15.6, 21.7, 6.5	13.44; 10.98	8.07; 5.68	A
14	3.39[a]	7.0, 12.0, 16.1, 8.4	13.68; 11.16	8.27; 5.59	B
20	3.58	6.2, 16.7, 13.7, 8.0, 16.3, 2.3	13.67; 10.98	8.28; 5.58	B
15	3.57	32.6, 2.3, 13.6, 17.3, 18.1, 17.3, 13.6, 2.3, 32.6	13.43; 11.18	7.96; 5.98	A

[a] These are approximate values due to the fact the the partially overlapping pyridine rings are not coplanar but their planes have an angle of 14.2 and 15.7°, for **12** and **14**, respectively. [b] See Figure 6.

0947-6539/01/0713-2802 $ 17.50+.50/0 *Chem. Eur. J.* **2001**, *7*, No. 13

slight but significant difference can be noted, which refers to the number of aromatic rings per turn and the exact relative positioning of overlapping rings. In the case of helical pentamer **12** and undecamer **15**, the overlap between ring n and ring $n+4$ is such that a carbon in β position of one pyridine ring coincides with another β carbon of the pyridine ring above (see top view in Figure 2a). This leads to a partial overlap of the aromatic rings. However, in the case of helical pentamer **14** and heptamer **20**, the helix is slightly more open. Carbons in α position of each pyridine ring coincide, leading to a very small overlap of the aromatic rings (see top view of Figure 2b). Instead, each aromatic ring lies above an amide group.

These differences may originate from crystal packing constraints. It may also be proposed that the Boc and Fmoc end-capping groups of **14** and **20** are responsible for a slight opening of the helical structures. These bulky groups are accommodated into the helices not by increasing the helical pitch, which would diminish favorable intramolecular stacking interaction, but by increasing the helix diameter.

Finally, the relative arrangement of the helices formed by undecamer **20** in the crystal deserves some comment. As shown in Figure 3, right- and left-handed individual helices are connected by two weak hydrogen bonds between terminal diamino-pyridine units, presenting both a nitrogen–nitrogen distance of 3.22 Å. These hydrogen bonds are likely to be responsible for the large dihedral angle (32.6°) formed between the most peripheral pyridine rings (Table 2). They lead to the propagation of the helical motif along one dimension in the form of a long alternatively right- and left-handed helical string. The hydrogen-bonded helices are offset, and their cavities are not superimposed along the string (Figure 3). Such well defined connected network of helices is not present in the crystal structures of compounds **12**, **14**, and **20**.

Single helix formation in solution: Dilute solutions of the oligomeric strands in $CDCl_3$ or $[D_6]DMSO$ feature sharp ^1H NMR spectra consistent with the presence of a single well defined species. In all cases, the pattern of signals indicate that on average, the molecular strands adopt a symmetrical structure with respect to the central pyridine ring. In this regard, the slight deviations from a perfect symmetry observed in the solid state for compounds **12**, **14**, and **20** may result from crystal packing constraints and not from a conformational preference.

The conformational behavior of heptamer **1** is described below as a representative example of the molecular strands in these solvents.[13] A partial assignment of the ^1H NMR spectrum of **1** shown in Figure 4 can be proposed on the basis of COSY experiments, and comparison with spectra of analogous compounds. In $CDCl_3$, the formation of intramolecular hydrogen bonds results in a strong deshielding of the corresponding protons, the signals of which appear at low field on the NMR spectra. Thus the signals of three of the four different amide hydrogens of heptamer **1** are seen at $\delta = 10.86$, 10.43, and 10.27. The terminal amide hydrogen is not involved in an intramolecular hydrogen bond; its signal appears at $\delta = 7.54$. Comparison of the spectrum of **1** to that of its shorter analogue trimer **8** shows that a number of signals are substantially shifted upfield, which suggests intramolecular stacking interactions in **1**. Signals of the most peripheral diamino-pyridine rings are at $\delta = 7.52$, 7.89 (H3 and H5) and 7.62 (H4) in **1**, whereas they are at $\delta = 7.90$, 8.01 (H3 and H5), and 7.72 (H4) in **8**. These latter values compare well with those of the more central diaminopyridine rings of **1**: $\delta = 7.89$, 8.18 (H3 and H5)

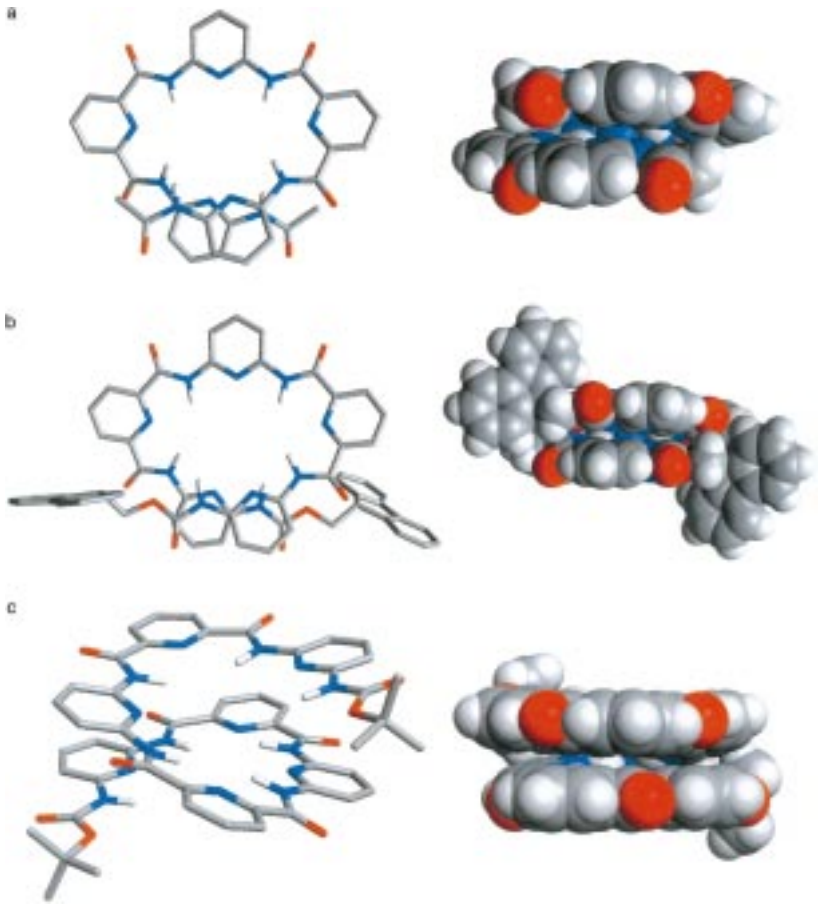

Figure 2. Top view (left) and side view (right) of the crystal structure of the single helix formed by a) pentamer **12** and b) pentamer **14**. c) Cylindrical bonds (left) and CPK representations (right) of the single helix formed by heptamer **20** in the crystal. Solvent molecules included in the crystal lattice and carbon hydrogens (in cylindrical bonds structures) are omitted for clarity. Where represented, hydrogen atoms have computer generated position.

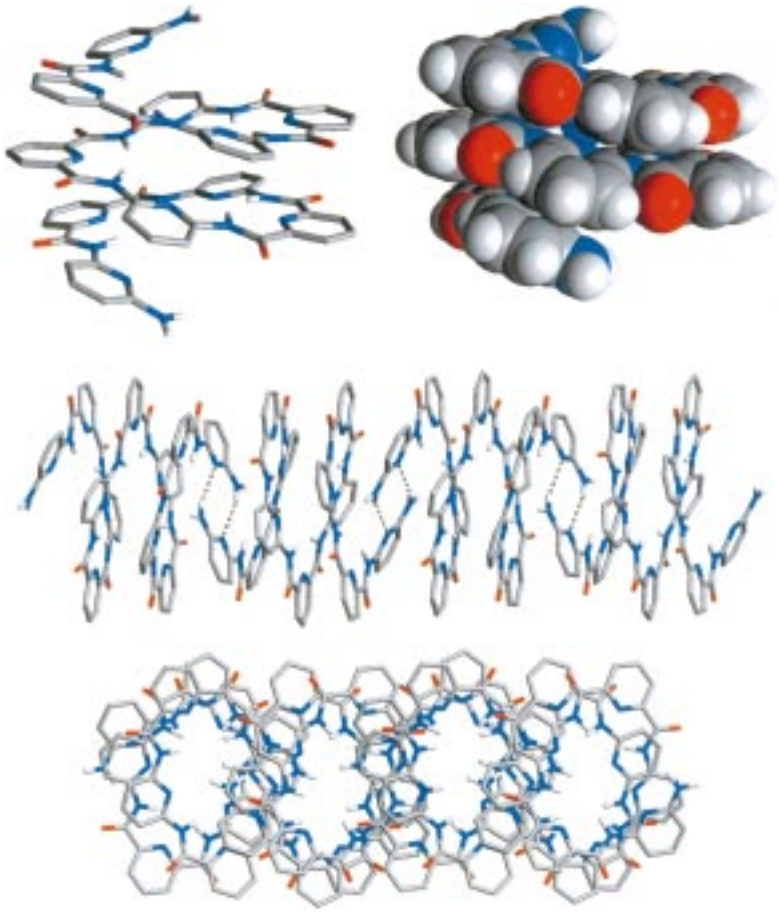

Figure 3. Cylindrical bonds and CPK representations of the single crystal structure of the helix formed by undecamer **15** (top). Solvent molecules included in the crystal lattice and carbon hydrogens (in cylindrical bonds structures) are omitted for clarity. Where represented, hydrogen atoms have computer generated position. A side view of the one-dimensional hydrogen-bonded networks formed by **15** is represented (center). Adjacent helices of opposite handedness are connected by two hydrogen bonds (dashed lines) between the peripheral diamino-pyridine units of the molecular strands. A top view of this hydrogen-bonded network (bottom) shows that the helices are not coaxial and that their cavities do not overlap.

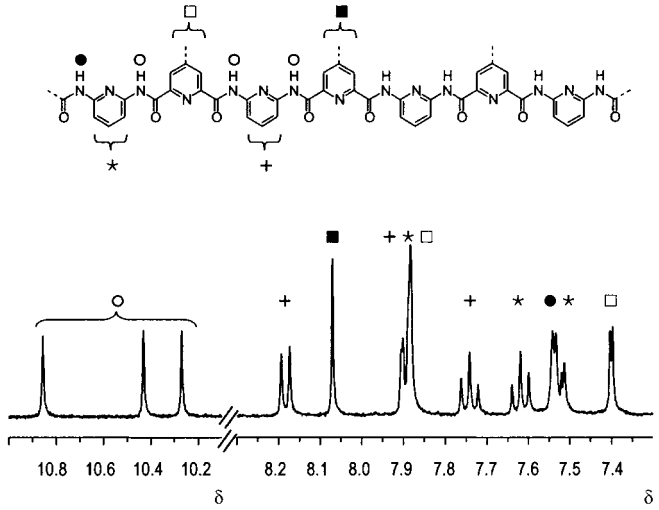

Figure 4. Part of the 400 MHz ^{1}H NMR spectrum of **1** at 0.9 mM in $CDCl_3$ at 25 °C. The partial assignement is based on COSY experiments, the values of the coupling constants, and on comparisons with ^{1}H NMR spectra of various precursors. The assignment of the spin systems of the two different diamino-pyridine rings is not unequivocal.

and 7.74 (H4). Signals of the second most peripheral pyridine rings are at $\delta = 7.40$ and 7.88 in **1**. This represents an almost 0.5 ppm difference despite the apparently symmetrical substitution of these rings. For comparison, the proton signal of the central pyridine ring of trimer **8** appears at $\delta = 7.92$. These data are consistent with a helical structure of heptamer **1** in solution involving an aromatic overlap between the most peripheral rings and part of the second most peripheral rings. Such an overlap would correspond well to the one and a half helical turn predicted by molecular modeling and observed in the solid state for heptamer **20**.

The folding of a nonchiral molecular strand into a chiral helix may result in diastereotopic patterns on the NMR spectra. This may be expected for the methylene protons belonging to the alkyl chains of **1**. However, no such signals were found in the spectra at room temperature, indicating that the right- and left-handed helices equilibrate rapidly on the NMR time scale, or that the chemical shift difference between signals of the potentially diastereomeric protons is very small. Low temperature experiments led to some broadening of the signals, but no splitting was observed even at -55 °C.

We also searched for NOESY contacts between remote atoms that may come in close proximity upon helix folding. However, NOESY spectra were complicated by correlation signals caused by exchange phenomena.[13] The correlation signals could not be assigned unequivocally to intramolecular contacts. The exchange results from the dimerization of the helices, presented in detail in the following article.[13b] It gives NOESY signals even at low concentration, when the dimer is present in minor amounts.

The folding of the strands into helices relies on intramolecular hydrogen bonding and aromatic stacking interactions which are both strong in low polar solvents such as $CDCl_3$. However, folding may not occur readily in polar solvents such as DMSO, which competes for hydrogen bonds. In Figure 5 the ^{1}H NMR spectra of [D_6]DMSO solutions of trimeric, pentameric, heptameric and undecameric strands are shown all having terminal pyridine-amino functions. In these compounds, strand curvature is expected to generate half a turn, one turn, one and a half, and two and a half turns, respectively. Taking the spectrum of the trimer as a reference,

0947-6539/01/0713-2804 $ 17.50+.50/0 *Chem. Eur. J.* **2001**, *7*, No. 13

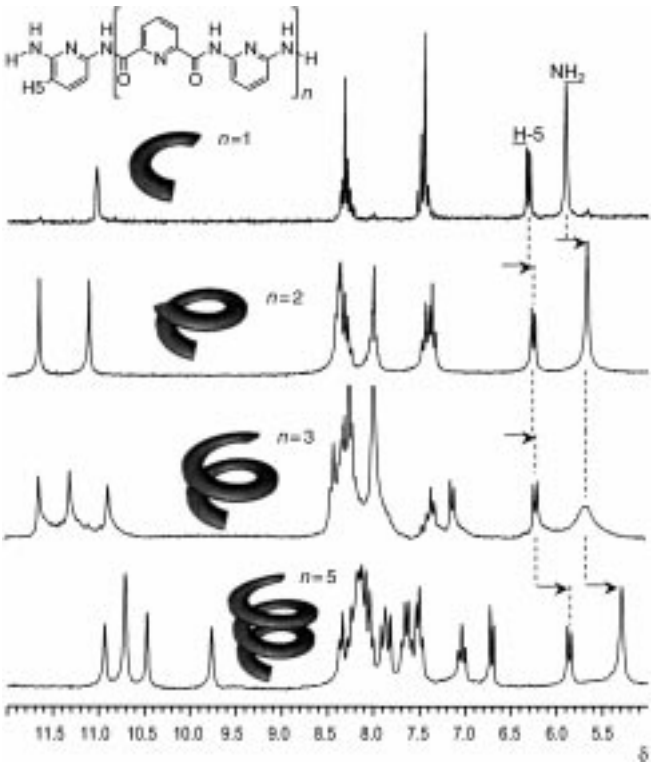

Figure 5. Part of the 200 MHz ^{1}H NMR spectra of trimeric, pentameric, heptameric, and undecameric molecular strands, having amino functions termini, in [D_6]DMSO at 25 °C. Whilst the trimer **10**, pentamer **11**, and undecamer **15** were synthesized and isolated compounds, the spectrum of the heptamer was simply obtained upon heating at 120 °C a [D_6]DMSO solution of its Boc protected analogue **20** which led to the deprotection of the terminal amino groups.

upfield shifts of the signals of the strands terminal functions are small for the pentamer and heptamer compared with what was observed in $CDCl_3$. Intramolecular aromatic stacking and thus helix formation are much less significant in [D_6]DMSO. For undecamer **15** in [D_6]DMSO, much larger upfield shifts of the hydrogen-bonded N*H*s and of the aromatic signals are observed (Figure 5), which suggests that a helical conformer is present. It is interesting to note that signals of the terminal NH_2 and *H*-5 are substantially more shifted than in the pentamer and heptamer. These protons should have similar environments regardless of the helix length. The variation of their chemical shifts thus suggests an increasing helix stability with increasing strand length.

Conformational energy and molecular dynamics simulations of single helix folding: In order to explore the mechanism of helix folding for these compounds, we performed conformational and molecular dynamics studies. The lowest energy conformers of heptamer **20** was calculated using the Monte-Carlo method under the MMFF94X force field on Spartan.[18] As expected, the helical conformer is the most stable. The second lowest energy conformers found also have a helical shape. They differ from the former by a about 180° rotation about one of the aryl–NH linkages on one of the terminal aromatic rings, which can occur without disruption of intramolecular hydrogen bonds. These rotations result in an over 20 kJ mol^{-1} additional conformational energy. The following more stable conformers combine two of such rotations, and are thus destabilized by over 40 kJ mol^{-1}, but still no hydrogen bonds are disrupted.

Stochastic molecular dynamics simulations were performed using the AMBER force field in MacroModel (see Experimental Section). A high energy linear heptameric conformer having two terminal acetamido functions was used as the initial structure. This local minimum was generated upon minimizing the completely extended structure using AMBER and the TNCG algorithm. The structure of this conformer is similar to the drawings of Schemes 1–3, and contains no hydrogen bonds. A series of dynamic simulations were undertaken over 1 to 3 ns at the same temperature of 300 K. Starting from several different quasi-linear conformers, folding of the linear conformer into a helical structure occurred in almost all cases. A representative 1.2 ns simulation is shown in Figure 6. In this case, folding occurs within approximately 500 ps, and the helix remains stable over the following 700 ps. During the simulations, rotations about the aryl–NH bonds were relatively frequent events. Rotations about the aryl–CO bonds usually occurred only once, which means that a formed hydrogen bond was rarely disrupted.

Conclusion

The present results provide an efficient approach to the programmed generation of helical superstructures through intramolecular self-organization directed by the structural and conformational features induced by the nonbonding interactions operating in a molecular strand. The design is based on a "pyridine-carboxamide" sequence which plays a helicity coding role analogous to that of the "pyridine–pyrimidine" helicity codon discovered earlier.[4] In particular, internal hydrogen bonding in the 2,6-dicarboxamide substituted pyridine rings induces curvature which leads to helical folding. Various structural modifications may be envisaged involving both the strand itself or appended groups decorating its exterior. Furthermore, the ability of the present molecular strands to dimerize opens the door to the design of a novel class of supramolecular double helices.[13]

Experimental Section

General methods: THF was distilled over sodium/benzophenone. Triethylamine (Lancaster, 99%) was used as received. 2,6-Diaminopyridine (Aldrich, 98%) was purified by recrystallization from hot chloroform after filtration with charcoal. Decanoyl chloride (Aldrich, 98%) and acetyl chloride (Aldrich, 98%) were distilled prior to use. Flash column chromatography was performed using silica gel (Geduran, SI 60 (40–63 mm, Merck). Infrared spectra were recorded as thin films on NaCl discs on a Perkin–Elmer 1600 Series FTIR. 400 MHz ^{1}H NMR spectra spectra were recorded on a Bruker Ultrashield Avance 400 spectrometer, 300 MHz ^{1}H NMR and and 75 MHz ^{13}C NMR spectra on a Bruker AM 300 spectrometer, and 200 MHz ^{1}H NMR and 50 MHz ^{13}C NMR spectra on a Bruker SY 200 spectrometer. The solvent signal was used as an internal reference for both ^{1}H and ^{13}C NMR spectra. The following notation is used for the ^{1}H NMR spectral splitting patterns: singlet (s), doublet (d), triplet (t), multiplet (m). FAB-mass spectrometric measurements were performed by the Service de Spectrométrie de Masse, Institut de Chimie, Université Louis Pasteur. Melting points (M.p.) were recorded on a Koffler Heizblock

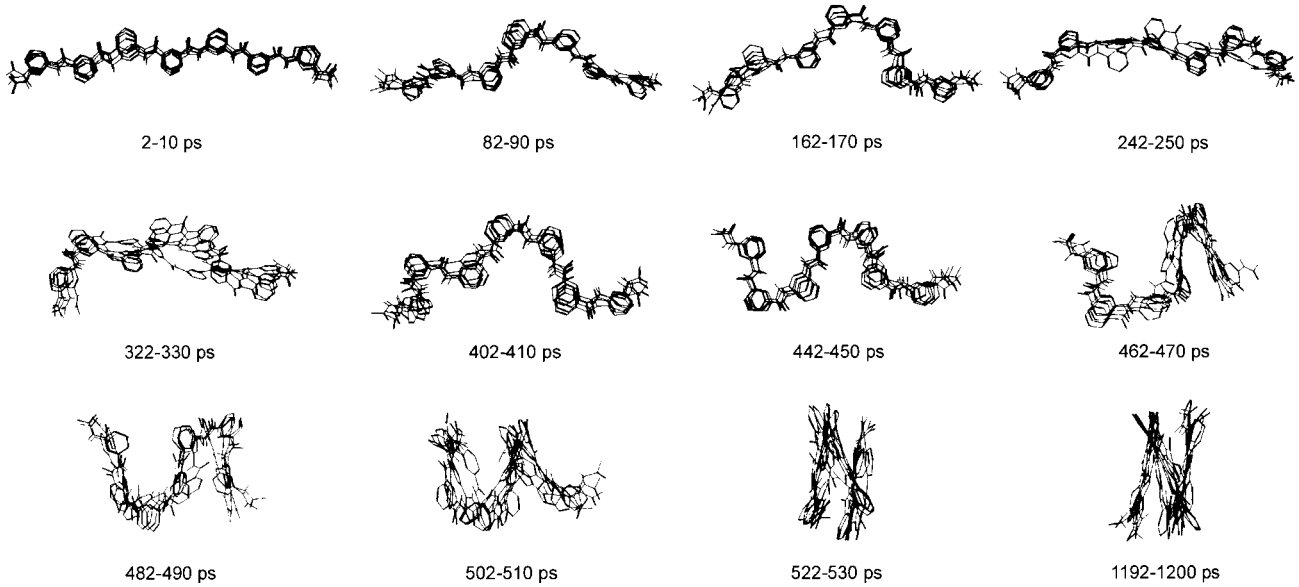

Figure 6. Stochastic dynamic simulation of an heptamer in chloroform over 1.2 ns. The initial linear strand is a local conformational energy minimum found upon minimizing an completely extended structure using AMBER force field on MacroModel. Snapshots are taken at different time intervals. In each case, five structures stored every 2 ps are superimposed. Conformers interconvert freely over the first 450 ps. Folding of the strand into a helical object occurs rapidly between 462 and 522 ps. The helix then remains stable until 1.2 ns, end of the calculation.

apparatus and are uncorrected. Elemental analyses were performed by the Service de Microanalyse, Institut de Chimie, Université Louis Pasteur.

X-ray crystallography: X-ray diffraction data for compounds **12**, **14**, and **20** were collected on a Nonius KappaCCD diffractometer with a graphite monochromatized $Mo_{K\alpha}$ radiation ($\lambda = 0.71071$ Å), ϕ scans, at 173 K, at the Laboratoire de Cristallochimie, Université Louis Pasteur, Strasbourg. As the crystals for compound **15** proved to be too small for analysis with conventional X-ray equipment, measurements were carried out at beamline *ID11* at the European Synchrotron Radiation Facility (ESRF) at Grenoble. A wavelength of 0.5040 Å was selected using a double crystal Si(*111*) monochromator, and data were collected using a Bruker "Smart" CCD-camera system at fixed 2θ. Data were reduced using the Bruker SAINT software. Their structure solution was determined using direct methods and refined (based on F^2 using all independent data) by full matrix least square methods (SHELXTL 97). Hydrogen atoms were included at calculated positions by using a riding model.

Crystallographic data (excluding structure factors) for the structures reported in this paper have been deposited with the Cambridge Crystallographic Data Centre as supplementary publication no. CCDC-147333 (**12**), CCDC-147334 (**14**), CCDC-147335 (**15**) and CCDC-142810 (**20**). Copies of the data can be obtained free of charge on application to CCDC, 12 Union Road, Cambridge CB2 1EZ, UK (fax: (+44) 1223 336–033; e-mail: deposit@ccdc.cam.ac.uk).

Molecular modeling: Lowest energy conformational search was performed on a MIPS R4400 Silicon Graphics workstation with Spartan (version 5.1.3, **1998**, Wavefunction, Inc.), using Monte-Carlo methods and MMFF94X force fields. Monte-Carlo uses a "simulated annealing" method to generate conformations of a molecule. Bonds and bent rings are randomly rotated whithin the molecule until a preferential (minimum energy) geometry is attained. The only external parameter that controls the search is temperature ($T = 5000$ K) that allows to jump energy barriers and to explore the whole potential energy surface.

Molecular dynamics simulations were performed on a R10000 O2 Silicon Graphics workstation using MacroModel version 6.5.[19] Stochastic dynamics[20] simulations were run in the MacroModel version of the AMBER*[15] force field at 300 K with GB/SA solvation[21] ($CHCl_3$), extended nonbonded distance cutoffs, constrained bond lengths, and a 1.5 fs timestep. After a 2 ps initialization period, structures were sampled every 2 ps for 1 to 3 ns.

4-Decyloxy-pyridine-2,6-dicarboxylic acid (3): Chelidamic acid (15 g, 81.9 mmol), 1-decanol (180 mL), toluene (70 mL), and H_2SO_4 were heated at 160 °C (bath temperature) during 20 h (2 mL) in a Dean–Stark apparatus. Toluene and decanol were then distilled off under vacuum. The residue was partitioned between hexane and aqueous sodium bicarbonate. The organic layer was dried ($MgSO_4$), filtered, concentrated, and passed through a short pad of silica gel eluting with EtOAc/hexane 5/95. The solvents were evaporated and the residue was added to a solution of KOH (85%, 30 g) in EtOH (1 L). The mixture was heated to reflux for 1 h with vigorous magnetic stirring. After cooling to room temperature, the precipitate was filtered and washed with EtOH. It was then dissolved in water. Some undissolved material was removed by filtration and the filtrate was acidified with CF_3CO_2H. The product precipitate was filtered off, washed with water and dried. Yield: 18.4 g (72%). M.p. >260 °C; IR (thin film): $\tilde{\nu} = 2953$, 2916, 2853, 1723, 1607, 1588, 1561, 1473, 1460, 1426, 1306, 1227, 1113, 1033, 1020, 932, 908, 888, 818, 793, 717, 695 cm^{-1}; ^1H NMR (200 MHz, TFA/[D$_6$]DMSO): $\delta = 8.26$ (s, 2H), 4.14 (t, $^3J = 6.5$ Hz, 2H), 2.02 (m, 2H), 1.30 (m, 14H), 0.88 (m, 3H); ^{13}C NMR (50 MHz, [D$_6$]DMSO): $\delta = 175.6$, 159.5, 141.0, 115.7, 73.6, 30.6, 28.1, 28.0, 27.8, 27.0, 24.2, 21.3, 11.6; FAB-MS: m/z (%): 322.2 (100) $[M-H]^-$; HRMS (FAB-MS): calcd for $[C_{17}H_{25}NO_5 - H]$: 323.1654; found: 322.1671.

4-Decyloxy-pyridine-2,6-dicarboxylic acid dimethyl ester (4): Diacid **3** (4 g) and $SOCl_2$ were heated to reflux for 1 h. After evaporation, the residue was dissolved in anhydrous toluene (50 mL), cooled to 0 °C, and MeOH (50 mL) was slowly added. The solution was allowed to stand 30 min at 0 °C, and 1 h at room temperature. It was then evaporated to dryness, and the product was recrystallised from EtOAc/hexane. Yield: 3.94 g (91%). M.p. 72–73 °C; IR (thin film): $\tilde{\nu} = 2947$, 2917, 2852, 1718, 1599, 1443, 1365, 1284, 1268, 1257, 1189, 1152, 1108, 1034, 991, 880, 787, 737 cm^-; ^1H NMR (200 MHz, $CDCl_3$): $\delta = 7.80$ (s, 2H), 4.14 (t, $^3J = 6.6$ Hz, 2H), 4.01 (s, 6H), 1.88 (m, 2H), 1.28 (m, 14H), 0.89 (t, $^3J = 6.5$ Hz, 3H); ^{13}C NMR (50 MHz, $CDCl_3$): $\delta = 167.1$, 165.2, 149.7, 114.5, 69.1, 53.2, 31.9, 29.5, 29.2, 28.7, 25.8, 22.6, 14.1; FAB-MS: m/z (%): 352.1 (100) $[M+H]^+$; HRMS (FAB-MS): calcd for $[C_{19}H_{29}NO_5+H]$: 352.2124; found: 352.2133.

4-Decyloxy-pyridine-2,6-dicarboxylic acid bis-[(6-amino-pyridin-2-yl)-amide] (6):[22] A 1.6 M solution of *n*BuLi (7.8 mmol, 4.88 mL, 670 mol%) in hexane was added at −78 °C to a solution of 2,6-diaminopyridine (**5**, 0.90 g, 8.1 mmol, 700 mol%) in dry THF (25 mL). After 20 min stirring at −78 °C, a solution of **4** (0.4 g, 1.14 mmol, 100 mol%) in dry THF (5 mL) was added dropwise. The reaction mixture was stirred at −78 °C for 8 h and then gradually warmed to r.t. and stirred over night. The reaction was then quenched with a 1 M solution of $NaHCO_3$ (25 mL) and extracted with EtOAc. The combined organic extracts were washed with sat. aq. brine and water, dried over $MgSO_4$, filtered, evaporated to dryness and purified using flash chromatography (silica gel, EtOAc/hexane 2:1) to afford **6** (0.190 g,

  0947-6539/01/0713-2806 $ 17.50+.50/0 *Chem. Eur. J.* **2001**, *7*, No. 13

40%) as a pale yellow powder. IR (thin film): $\tilde{\nu}$ = 3449, 3358, 3210, 2959, 2872, 1689, 1622, 1600, 1537, 1451, 1342, 1300, 1249, 1127, 1064, 1030, 878, 791 cm^{-1}; ^{1}H NMR (200 MHz, [D$_6$]DMSO): δ = 10.04 (brs, 2H), 7.94 (s, 2H), 7.76 (d, ^3J = 7.9 Hz, 2H), 7.52 (t, ^3J = 7.9 Hz, 2H), 6.29 (d, ^3J = 8.0 Hz, 2H), 4.71 (brs, 4H), 4.17 (t, ^3J = 6.5 Hz, 2H), 1.81 (m, 2H), 1.25 (m, 14H), 0.84 (t, J = 6.4 Hz, 3H); ^{13}C NMR (75 MHz, [D$_6$]DMSO): δ = 168.1, 161.7, 157.7, 150.4, 148.8, 139.9, 111.7, 105.1, 103.5, 69.0, 31.6, 29.3, 29.0, 28.5, 25.6, 22.4, 13.8; FAB-MS: m/z (%): 506.3 (100) [M+H]$^+$; elemental analysis calcd (%) for $C_{27}H_{35}N_7O_3$ (505.61): C 64.14, H 6.98; found: C 64.21, H 7.09.

4-Decyloxy-pyridine-2,6-dicarboxylic acid 2-[(6-amino-pyridin-2-yl)-amide] 6-[(6-decanoylamino-pyridin-2-yl)-amide] (7) and **4-decyloxy-pyridine-2,6-dicarboxylic acid bis-[(6-decanoylamino-pyridin-2-yl)-amide] (8)**: Decanoyl chloride (0.0482 g, 0.253 mmol, 80 mol%) was added at 0°C using a microsyringe to a solution of **6** (0.160 g, 0.316 mmol, 100 mol%) and triethylamine (0.032 g, 0.316 mmol, 100 mol%) in dry THF (5 mL) and the reaction stirred for 30 min, before warming to r.t. The reaction mixture was filtered, evaporated to dryness and applied to a column (silica gel, EtOAc/hexane 1:2) to provide **7** (0.065 g, 32%). Under these conditions, the amount of undesired side product **8** (0.025 g, 10%) was relatively small and the unreacted starting material **6** could be recovered.

Compound **7**: Yellowish powder. M.p. 81–83°C; IR (thin film): $\tilde{\nu}$ = 3341, 2923, 2861, 1694, 1585, 1532, 1462, 1342, 1294, 1241, 1151, 1037, 798 cm^{-1}; ^{1}H NMR (200 MHz, CDCl$_3$): δ = 10.33 (brs, 1H), 10.26 (brs, 1H), 9.08 (brs, 1H), 8.07 (d, ^3J = 8.3 Hz, 1H), 8.02 (d, ^3J = 8.7 Hz, 1H), 7.92 (s, 1H), 7.91 (s, 1H), 7.76 (t, ^3J = 8.1 Hz, 1H), 7.68 (d, ^3J = 7.9 Hz, 1H), 7.52 (t, ^3J = 8.0 Hz, 1H), 6.28 (d, ^3J = 7.9 Hz, 1H), 4.92 (brs, 2H), 4.16 (t, ^3J = 6.5 Hz, 2H), 2.44 (t, ^3J = 7.4 Hz, 2H), 2.15 (t, ^3J = 7.6 Hz, 2H), 1.81 (m, 2H), 1.71 (m, 2H), 1.24 (m, 24H), 0.86 (brs, 6H); ^{13}C NMR (50 MHz, CDCl$_3$): δ = 179.4, 172.6, 168.4, 161.5, 157.5, 150.3, 148.8, 141.1, 141.0, 112.0, 110.3, 109.6, 105.3, 103.4, 69.3, 37.5, 34.3, 31.9, 29.5, 29.4, 29.3, 29.2, 29.0, 28.7, 25.8, 25.4, 24.7, 22.6, 14.1; FAB-MS: m/z (%): 660.3 (100) [M+H]$^+$; HRMS (FAB-MS): calcd for [$C_{37}H_{53}N_7O_4$+H]: 660.4237; found: 660.4228.

Side product **8**: ^{1}H NMR (200 MHz, CDCl$_3$): δ = 10.19 (brs, 2H), 8.42 (brs, 2H), 8.01 (d, ^3J = 7.5 Hz, 2H), 7.92 (s, 2H), 7.90 (d, ^3J = 7.7 Hz, 2H), 7.72 (t, ^3J = 8.0 Hz, 2H), 4.15 (t, ^3J = 6.6 Hz, 2H), 2.39 (t, ^3J = 7.4 Hz, 4H), 1.85 (m, 2H), 1.71 (m, 4H), 1.27 (brs, 38H), 0.87 (brs, 9H); FAB-MS: m/z (%): 814.5 (100) [M]$^+$; elemental analysis calcd (%) for $C_{47}H_{71}N_7O_5$ (814.11): C 69.34, H 8.79; found: C 69.14, H 8.89.

4-Decyloxy-pyridine-2,6-dicarboxylic acid bis-[(6-{[6-(6-decanoylamino-pyridin-2-ylcarbamoyl)-4-decyloxy-pyridine-2-carbonyl]-amino}-pyridin-2-yl)-amide] (1): Previously prepared crude diacid chloride **3b** (0.118 g, 0.300 mmol, 55 mol%) was dissolved in dry toluene (2 mL) and immediately transferred through syringe to a previously prepared solution of mono-amine **7** (0.444 g, 0.545 mmol, 100 mol%) and triethylamine (0.066 g, 0.654 mmol, 120 mol%) in toluene (10 mL) at 0°C. The reaction was allowed to proceed for 30 min, upon which time the reaction mixture was filtered, evaporated to dryness and the residue purified by column chromatography (silica gel, 1% MeOH/CH_2Cl_2). The collected fractions were evaporated and dried on high vacuum. Compound **1** (0.342 g, 78%) was obtained as a pale grey gluey solid. M.p. 255–258°C; IR (thin film): $\tilde{\nu}$ = 3462, 3325, 2922, 2852, 1694, 1592, 1520, 1463, 1345, 1305, 1248, 1210, 1159, 1117, 1037, 1000, 878, 799, 721 cm^{-1}; ^{1}H NMR (400 MHz, CDCl$_3$, 0.9 mM, monomer): δ = 10.86 (s, 2H), 10.43 (s, 2H), 10.27 (s, 2H), 8.18 (d, ^3J = 7.9 Hz, 2H), 8.07 (s, 2H), 7.89 (m, 6H), 7.74 (t, ^3J = 7.9 Hz, 2H), 7.62 (t, ^3J = 8.3 Hz, 2H), 7.54 (d, ^4J = 3.2 Hz, 2H), 7.52 (d, ^4J = 3.2 Hz, 1H), 7.40 (d, ^4J = 2.5 Hz, 2H), 4.25 (m, 6H), 1.95 (m, 10H), 1.30 (m, 75H), 0.89 (t, ^3J = 7.0 Hz, 6H), 0.86 (t, ^3J = 7.0 Hz, 9H); ^{13}C NMR (400 MHz, CDCl$_3$, 1 mM, monomer): δ = 171.2, 169.2, 168.5, 161.5, 160.8, 150.6, 150.5, 149.7, 149.6, 149.4, 149.1, 148.9, 142.0, 141.4, 112.7, 112.1, 110.7, 110.5, 110.0, 109.7; FAB-MS: m/z (%): 1606.9 (90) [M]$^+$; elemental analysis calcd (%) for $C_{91}H_{127}N_{15}O_{11}$ (1607.08): C 68.01, H 7.97; found: C 67.98, H 8.24.

Pyridine-2,6-dicarboxylic acid bis-[(6-amino-pyridin-2-yl)-amide] (10) and **2,6-bis-{[6-(6-amino-pyridin-2-ylcarbamoyl)-pyridine-2-carbonyl]-amino}-pyridine (11)**: A 1.6M solution of nBuLi (0.158 mol, 95 mL) in hexane was added dropwise to a solution of 2,6-diaminopyridine (**5**, 17.85 g, 0.164 mol, 700 mol%) in dry THF (300 mL, 1M) at −78°C. After stirring for 20 min at −78°C, a solution of dimethyl pyridine-2,6-dicarboxylate (**9**, 4.6 g, 24 mmol, 100 mol%) in dry THF (50 mL) was added portionwise. The reaction mixture was stirred at −78°C for 12 h, gradually warmed to r.t. and stirred over night. The reaction was quenched with EtOAc, then MeOH at r.t. The combined organic extracts were evaporated to dryness and purified several times using flash chromatography (silica gel, gradient 5% hexane/EtOAc → 100% EtOAc) to afford **10** (1.5 g, 18%) as a yellow solid. As a side product of the reaction, **11** (0.5 g, 4%) was obtained. Compound **10**: M.p. >260°C; IR (thin film): $\tilde{\nu}$ = 3306, 2832, 1677, 1614, 1570, 1518, 1444, 1298, 1241, 1139, 1063, 1002, 978, 789 cm^{-1}; ^{1}H NMR (200 MHz, [D$_6$]DMSO): δ = 11.03 (brs, 2H), 8.32 (m, 3H), 7.45 (brs, 4H), 6.31 (d, ^3J = 6.8 Hz, 2H), 5.90 (brs, 4H); ^{13}C NMR (50 MHz, [D$_6$]DMSO): δ = 162.0, 158.6, 149.5, 149.0, 139.6, 139.0, 125.2, 104.3, 102.0; FAB-MS: m/z (%): 350.1 (100) [M+H]$^+$; elemental analysis calcd (%) for $C_{17}H_{15}N_7O_2$ (349.34): C 58.45, H 4.33, N 28.07; found: C 58.21, H 4.08, N 28.30.

Compound **11**: M.p. >260°C; IR (thin film): $\tilde{\nu}$ = 3431, 3360, 3210, 2959, 2863, 1694, 1621, 1580, 1532, 1463, 1311, 1246, 1144, 1073, 1001, 898, 790 cm^{-1}; ^{1}H NMR (200 MHz, [D$_6$]DMSO): δ = 11.66 (brs, 2H), 11.11 (brs, 2H), 8.36 (m, 6H), 8.00 (brs, 3H), 7.40 (brs, 4H), 6.26 (d, ^3J = 7.5 Hz, 2H), 5.67 (brs, 4H); ^{13}C NMR (50 MHz, [D$_6$]DMSO): δ = 162.7, 162.1, 158.6, 150.0, 149.5, 149.3, 148.7, 140.2, 139.7, 138.9, 125.7, 125.5, 112.5, 104.5, 102.9; FAB-MS: m/z (%): 590.4 (100) [M+H]$^+$; elemental analysis calcd (%) for $C_{29}H_{23}N_{11}O_4$ (589.56)·[H_2O]$_2$: C 55.88, H 4.35, N 24.63; found: C 56.06, H 4.61, N 22.81.

2,6-Bis-{[6-(6-acetylamino-pyridin-2-ylcarbamoyl)-pyridine-2-carbonyl]-amino}-pyridine (12): A solution of **11** (25 mg, 0.0424 mmol, 100 mol%) and triethylamine (9.4 mg, 0.0933 mmol, 220 mol%) were dissolved in a minimal amount of dry THF (1 mL), and acetyl chloride (7.0 mg, 6.3 μL, 0.0891 mmol, 210 mol%) added through a dry syringe at r.t. The reaction was stirred for 2 h, filtered, evaporated to dryness and applied to a column of silica (silica gel, 5% EtOH/EtOAc). Compound **12** (24 mg, 84%) was obtained as a white solid. M.p. >260°C; IR (thin film): $\tilde{\nu}$ = 3317, 2923, 1701, 1690, 1582, 1508, 1452, 1306, 1241, 1157, 1073, 1002, 798 cm^{-1}; ^{1}H NMR (200 MHz, [D$_6$]DMSO): δ = 11.32 (brs, 2H), 11.04 (brs, 2H), 10.06 (brs, 2H), 8.39 (m, 6H), 8.02 (m, 3H), 7.76 (m, 6H), 1.93 (s, 6H); ^{13}C NMR (50 MHz, [D$_6$]DMSO): δ = 169.0, 162.5, 162.0, 150.6, 149.9, 148.7, 140.1, 125.7, 112.2, 110.5, 109.9, 23.7; FAB-MS: m/z (%): 674.3 (100) [M+H]$^+$; HRMS (FAB-MS): calcd for [$C_{33}H_{27}N_{11}O_6$+H]: 674.2224; found: 674.2225. Crystallographic data (single helix) in Table 1.

(6-{[6-(6-{[6-(6-Amino-pyridin-2-ylcarbamoyl)-pyridine-2-carbonyl]-amino}-pyridin-2-ylcarbamoyl)-pyridine-2-carbonyl]-amino}-pyridin-2-yl)-carbamic acid 9*H*-fluoren-9-ylmethyl ester (13) and **2,6-bis-({6-[6-(9*H*-fluoren-9-ylmethoxycarbonylamino)-pyridin-2-ylcarbamoyl]-pyridine-2-carbonyl}-amino)-pyridine (14)**:[23] **11** (121.0 mg, 0.2052 mmol, 100 mol%) and triethylamine (24.9 mg, 0.2462 mmol, 120 mol%) were dissolved in the minimal amount of dry THF (15 mL). FmocCl (63.7 mg, 0.2462 mmol, 120 mol%), dissolved in THF (1.5 mL), was added dropwise at r.t., and the mixture stirred for 2.5 h. The mixture was evaporated to dryness without filtration, applied to a column of silica gel, and the product fractions collected. (silica gel, 4% EtOAc/CH_2Cl_2 (to eliminate solvent front impurities), then gradient EtOAc → 4% EtOH/EtOAc). Compound **13** (41 mg, 25%) and **14** (19 mg, 9%) were obtained as white solids. Unreacted **11** (45 mg, 37%) could be recovered. Compound **13**: M.p. >175°C (decomp); IR (thin film): $\tilde{\nu}$ = 3317, 2911, 1738, 1694, 1623, 1582, 1530, 1510, 1454, 1306, 1247, 1211, 1151, 074, 995, 797 cm^{-1}; ^{1}H NMR (200 MHz, CDCl$_3$): δ = 10.41 (brs, 1H), 10.34 (brs, 1H), 10.31 (brs, 1H), 10.16 (brs, 1H), 8.36 (d, ^3J = 7.7 Hz, 1H), 8.20 (m, 3H), 8.00 (t, ^3J = 7.8 Hz, 1H), 7.87 (m, 4H), 7.59 (m, 4H), 7.24 (m, 8H), 6.86 (t, ^3J = 8.0 Hz, 1H), 5.64 (d, ^3J = 7.9 Hz, 1H), 4.97 (brs, 2H), 4.01 (d, ^3J = 7.2 Hz, 2H), 3.78 (t, ^3J = 7.1 Hz, 1H); ^{13}C NMR (500 MHz, CDCl$_3$): δ = 165.6, 161.3, 160.7, 152.0, 151.5, 150.4, 149.3, 148.8, 148.2, 148.1, 147.8, 147.6, 143.3, 140.9, 140.8, 140.4, 139.3, 139.1, 127.5, 126.8, 125.9, 125.7, 125.6, 125.3, 124.9, 119.7, 110.7, 110.6, 108.7, 107.9, 106.8, 104.5, 103.3, 67.1, 46.5; FAB-MS: m/z (%): 812.3 (100) [M+H]$^+$; HRMS (FAB-MS): calcd for [$C_{44}H_{33}N_{11}O_6$+H]: 812.2694; found: 812.2700.

Compound **14**: M.p. >180°C (decomp); IR (thin film): $\tilde{\nu}$ = 3370, 3318, 2923, 2852, 1741, 1698, 1586, 1514, 1452, 1396, 1307, 1247, 1209, 1160, 1074, 1002, 909, 841, 799, 739 cm^{-1}; ^{1}H NMR (200 MHz, CDCl$_3$): δ = 10.20 (brs, 2H), 9.96 (brs, 2H), 8.39 (d, ^3J = 7.2 Hz, 2H), 8.17 (d, ^3J = 8.1 Hz, 2H), 8.06 (d, ^3J = 7.6 Hz, 2H), 7.88 (d, ^3J = 7.8 Hz, 2H), 7.75 (d, ^3J = 9.1 Hz, 2H), 7.62 (d, ^3J = 7.5 Hz, 4H), 7.37 (t, ^3J = 7.9 Hz, 1H), 7.29 (m, 12H), 7.05 (t, ^3J = 7.3 Hz, 4H), 4.00 (d, ^3J = 7.1 Hz, 4H), 3.81 (t, ^3J = 7.0 Hz, 2H); ^{13}C NMR (50 MHz, CDCl$_3$): δ = 161.3, 160.9, 152.1, 149.7, 149.3, 148.9, 148.1, 143.3, 141.1, 140.9, 139.4, 127.7, 127.0, 126.0, 125.5, 124.9, 123.7, 119.9, 110.7, 108.7,

108.1, 67.2, 46.6; FAB-MS: *m/z* (%): 1034.4 (100) $[M+H]^+$. Crystallographic data of **14** (single helix) in Table 1.

2,6-Bis-(6-{[6-(6-{[6-(6-amino-pyridin-2-ylcarbamoyl)-pyridine-2-carbonyl]-amino}-pyridin-2-ylcarbamoyl)-pyridine-2-carbonyl]-amino}-pyridin-2-ylcarbamoyl)-pyridine (15): A previously prepared diacid chloride **16b** solution in THF was cannulated portionwise to **13** (32.0 mg, 0.0394 mmol, 200 mol%) and triethylamine (8.7 mg, 0.0870 mol, 220 mol%), dissolved in dry THF (4 mL). The reaction was complete by TLC after the addition of 140 mol% of **16b** at r.t. after 30 min. The mixture was then filtered and evaporated to dryness. The intermediately obtained *2,6-bis-(6-{[6-(6-{[6-(6-{9H-fluoren-9-ylmethoxycarbonylamino}-pyridin-2-ylcarbamoyl)-pyridine-2-carbonyl]-amino}-pyridin-2-ylcarbamoyl)-pyridine-2-carbonyl]-amino}-pyridin-2-ylcarbamoyl)-pyridine* was deprotected[23] without further purification by dissolving in DMF (1 mL) and addition of piperidine (100 μL) and stirring at r.t. for 1 h. The white precipitate, diamine **15** (18 mg, 70%) was filtered, washed with small amounts of DMF, ethanol and chloroform, and dried under high vacuum. M.p. $>260\,^{\circ}C$; ^1H NMR (200 MHz, hot [D$_6$]DMSO): $\delta = 10.94$ (brs, 2H), 10.72 (brs, 4H), 10.47 (brs, 2H), 9.77 (brs, 2H), 8.35 (d, $^3J = 7.2$ Hz, 2H), 8.15 (m, 14H), 7.89 (d, $^3J = 8.3$ Hz, 2H), 7.84 (d, $^3J = 8.2$ Hz, 2H), 7.66 (t, $^3J = 7.7$ Hz, 2H), 7.63 (t, $^3J = 7.6$ Hz, 2H), 7.51 (t, $^3J = 6.9$ Hz, 3H), 7.04 (t, $^3J = 7.9$ Hz, 2H), 6.71 (d, $^3J = 7.9$ Hz, 2H), 5.86 (d, $^3J = 7.8$ Hz, 2H), 5.29 (brs, 4H); FAB-MS: *m/z* (%): 1310.4 (25) $[M]^+$. Crystallographic data (single helix) in Table 1.

(6-Amino-pyridin-2-yl)-carbamic acid *tert*-butyl ester (17):[24] LiHMDS (15.39 g, 0.092 mol, 200 mol%), dissolved in dry THF (80 mL) was added dropwise over a period of 15 min to a solution of diaminopyridine (**5**, 5.00 g, 0.046 mol, 100 mol%) in dry THF (50 mL). After further 10 min a soluttion of di-*tert*-butyldicarbonate (10.03 g, 0.046 mol, 100 mol%) in THF (30 mL) was added dropwise during 20 min and the reaction allowed to proceed at r.t. for further 3 h. Removal of the solvent and purification of the reaction residue by column chromatography (silica gel, 30% EtOAc/CH_2Cl_2) afforded **17** (5.51 g, 57%) in an overstatistical quantity as a white powder. M.p. 125–127 °C; IR (thin film): $\tilde{\nu} = 3379$, 3211, 2978, 1720, 1619, 1578, 1529, 1457, 1423, 1392, 1368, 1298, 1235, 1158, 1085, 1053, 951, 886, 790, 760, 729 cm^{-1}; ^1H NMR (200 MHz, $CDCl_3$): $\delta = 8.08$ (brs, 1H), 7.39 (t, $^3J = 8.0$ Hz, 1H), 7.20 (d, $^3J = 8.0$ Hz, 1H), 6.14 (d, $^3J = 7.9$ Hz, 1H), 4.51 (brs, 2H), 1.50 (s, 9H); ^{13}C NMR (50 MHz, $CDCl_3$): $\delta = 157.3$, 152.6, 150.7, 139.8, 102.9, 101.8, 80.8, 28.3; FAB-MS: *m/z* (%): 210.1 (100) $[M+H]^+$; elemental analysis calcd (%) for $C_{10}H_{15}N_3O_2$ (209.24): C 57.40, H 7.23, N 20.08; found: C 57.10, H 7.47, N 19.94.

2,6-Bis-(6-*tert*-butoxycarbonylamino-pyridin-2-ylcarbamoyl)-pyridine (18): Compund **17** (5.00 g, 0.0239 mol, 200 mol%) and triethylamine (2.66 g, 0.0263 mol, 220 mol%) were dissolved in dry THF (90 mL) and previously prepared diacid chloride **16b** (2.44 g, 0.0120 mol, 100 mol%) in THF (10 mL) was added dropwise at r.t. The reaction was allowed to proceed for further 1 h at r.t. The reaction mixture was then filtered, evaporated to dryness and applied to a column of silica (silica gel, 20% EtOAc/CH_2Cl_2). Compound **18** (5.75 g, 88%) was obtained as a white powder. M.p. $>210\,^{\circ}C$ (decomp); IR (thin film): $\tilde{\nu} = 3365$, 3300, 2979, 2923, 1731, 1696, 1584, 1504, 1461, 1392, 1388, 1297, 1230, 1155, 1074, 1000, 881, 842, 800, 753 cm^{-1}; ^1H NMR (200 MHz, [D$_6$]DMSO): $\delta = 11.13$ (brs, 2H), 9.45 (brs, 2H), 8.37 (m, 3H), 7.83 (brs, 4H), 7.60 (dd, $^3J = 6.4$ Hz, $^4J = 2.4$ Hz, 2H), 1.43 (s, 18H); ^{13}C NMR (50 MHz, [D$_6$]DMSO): $\delta = 162.1$, 152.5, 151.0, 149.3, 148.6, 140.0, 139.9, 125.6, 109.5, 109.0, 79.7, 27.9; FAB-MS: *m/z* (%): 550.2 (45) $[M+H]^+$; elemental analysis calcd (%) for $C_{27}H_{31}N_7O_6$ (549.58): C 59.01, H 5.69, N 17.84; found: C 59.19, H 5.78, N 18.00.

(6-{[6-(6-Amino-pyridin-2-ylcarbamoyl)-pyridine-2-carbon-yl]-amino}-pyridin-2-yl)-carbamic acid *tert*-butyl ester (19):[25] TMSI (0.741 g, 0.53 mL, 3.703 mmol, 110 mol%) was added through a dry syringe to **18** (1.85 g, 3.366 mmol, 100 mol%) dissolved in chloroform (20 mL) and the mixture stirred at r.t. for 30 min. The solvent was then evaporated, the residue dissolved in methanol (30 mL) and heated to reflux for 45 min to hydrolyse the intermediately formed trimethylsilyloxycarbonyl group. After evaporation of the solvent, the solid residue was applied to a column of silica (silica gel, gradient 20% EtOAc/CH_2Cl_2 → 50% EtOAc/CH_2Cl_2). Compound **19** (0.92 g, 61%) was obtained as a white powder. M.p. 135–136 °C; IR (thin film): $\tilde{\nu} = 3366$, 3292, 2977, 1730, 1692, 1617, 1582, 1533, 1453, 1392, 1367, 1300, 1233, 1154, 1073, 1001, 884, 793, 748 cm^{-1}; ^1H NMR (200 MHz, [D$_6$]DMSO): $\delta = 11.28$ (brs, 1H), 11.15 (brs, 1H), 9.53 (brs, 1H), 8.35 (m, 3H), 7.84 (m, 2H), 7.60 (m, 2H), 7.33 (d, $^3J = 7.7$ Hz, 1H), 7.42 (d, $^3J = 8.1$ Hz, 1H), 1.48 (s, 9H); ^{13}C NMR (50 MHz, [D$_6$]DMSO): $\delta = 161.7$, 161.2, 157.6, 152.5, 150.6, 148.8, 148.3, 139.7, 139.0, 125.5, 125.3, 108.5, 108.1, 104.6, 102.7, 100.0, 80.3, 27.6; FAB-MS: *m/z* (%): 450.1 (70) $[M+H]^+$; elemental analysis calcd (%) for $C_{22}H_{23}N_7O_4$ (449.46)·$[H_2O]_2$: C 54.42, H 5.61, N 20.20; found: C 54.62, H 5.31, N 20.09.

2,6-Bis-(6-{[6-(6-*tert*-butoxycarbonylamino-pyridin-2-ylcarbamoyl)-pyridine-2-carbonyl]-amino}-pyridin-2-ylcarbamoyl)-pyridine (20): The previously prepared diacid chloride **16b** (0.163 g, 0.59 mmol, 100 mol%) solution in THF (2 mL) was cannulated at r.t to a solution of **19** (0.530 g, 1.18 mmol, 200 mol%) and triethylamine (0.131 g, 1.30 mmol, 220 mol%) in dry THF (30 mL). The reaction was allowed to proceed for 1 h at r.t, upon which time 0.3 equiv of **16b** was added to compensate for hydrolysis. After another 30 min, the reaction mixture was filtered, evaporated to dryness and chromatographed on a column of silica (silica gel, 5% EtOH/$CHCl_3$) to afford **20** (0.370 g, 61%) as a white powder. M.p. $>250\,^{\circ}C$; IR (thin film): $\tilde{\nu} = 3318$, 2971, 1731, 1703, 1582, 1510, 1454, 1392, 1388, 1306, 1229, 1155, 1073, 1002, 800 cm^{-1}; ^1H NMR (200 MHz, [D$_6$]DMSO): $\delta = 11.17$ (brs, 2H), 10.62 (brs, 2H), 10.34 (brs, 2H), 9.44 (brs, 2H), 8.56 (d, $^3J = 7.8$ Hz, 2H), 8.33 (m, 6H), 8.21 (d, $^3J = 6.8$ Hz, 2H), 8.02 (d, $^3J = 6.8$ Hz, 2H), 7.93 (m, 3H), 7.61 (t, $^3J = 7.8$ Hz, 2H), 7.48 (d, $^3J = 7.8$ Hz, 2H), 7.31 (d, $^3J = 7.8$ Hz, 2H), 1.29 (s, 18H); ^{13}C NMR (50 MHz, $CDCl_3$, 65 mM, dimer): $\delta = 199.1$, 160.6, 160.5, 150.9, 149.9, 149.6, 148.7, 147.7, 140.9, 140.4, 140.1, 139.5, 136.7, 125.9, 125.3, 110.1, 109.8, 108.5, 108.1, 107.2, 81.0, 27.8; FAB-MS: *m/z* (%): 1030.3 (65) $[M]^+$, 2060.7 (3) $[M_2]^+$; elemental analysis calcd (%) for $C_{51}H_{47}N_{15}O_{10}$ (1030.01): C 59.47, H 4.60, N 20.40; found: C 59.62, H 4.86, N 20.14. Crystallographic data of **20** (single helix) in Table 1.

Acknowledgements

This work was supported by the CNRS, by a predoctoral fellowship (V.B.) from the Forschungszentrum Karlsruhe GmbH, Germany, and by a NSF-NATO postdoctoral fellowship (R.G.K.). We thank M. Laguerre and E. Ruiz for assistance with molecular dynamics simulations and lowest energy conformational searches, respectively, and A. DeCian and J. Fischer for the use of their X-ray diffraction facilities at ULP, Strasbourg. We also thank G. Vaughan for the measurements at the ESRF in Grenoble.

[1] a) A. E. Rowan, R. J. M. Nolte, *Angew. Chem.* **1998**, *110*, 65; *Angew. Chem. Int. Ed.* **1998**, *37*, 63; b) T. Katz, *Angew. Chem.* **2000**, *112*, 1997; *Angew. Chem. Int. Ed.* **2000**, *39*, 1921.

[2] a) Y. Hamuro, J. S. Geib, A. D. Hamilton, *J. Am. Chem. Soc.* **1997**, *119*, 10587; b) Y. Hamuro, J. S. Geib, A. D. Hamilton, *Angew. Chem.* **1994**, *106*, 465; *Angew. Chem. Int. Ed. Engl.* **1994**, *33*, 446; c) J. Zhu, R. D. Parra, H. Zeng, E. Skrzypczak-Jankun, X. C. Zeng, B. Gong, *J. Am. Chem. Soc.* **2000**, *122*, 4219.

[3] a) D. Seebach, M. Overhand, F. N. M. Kühnle, B. Martinoni, L. Oberer, U. Hommel, H. Widmer, *Helv. Chim. Acta* **1996**, *79*, 913; b) D. Seebach, P. E. Ciceri, M. Overhand, B. Jaun, D. Rigo, L. Oberer, U. Hommel, R. Amstutz, H. Widmer, *Helv. Chim. Acta* **1996**, *79*, 2043; c) D. H. Appella, L. A. Christianson, D. A. Klein, M. R. Richards, D. R. Powell, S. H. Gellman, *J. Am. Chem. Soc.* **1999**, *121*, 7574.

[4] a) G. S. Hanan, J.-M. Lehn, N. Kyritsakas, J. Fischer, *J. Chem. Soc. Chem. Commun.* **1995**, 765; b) D. Bassani, J.-M. Lehn, G. Baum, D. Fenske, *Angew. Chem.* **1997**, *109*, 1931; *Angew. Chem. Int. Ed. Engl.* **1997**, *36*, 1845; c) D. Bassani, J.-M. Lehn, *Bull. Soc. Chim. Fr.* **1997**, *134*, 897; d) M. Ohkita, J.-M. Lehn, G. Baum, D. Fenske, *Chem. Eur. J.* **1999**, *5*, 3471.

[5] L. A. Cuccia, J.-M. Lehn, J.-C. Homo, M. Schmutz, *Angew. Chem.* **2000**, *112*, 239; *Angew. Chem. Int. Ed.* **2000**, *37*, 233.

[6] F. R. Heirtzler, M. Neuburger, M. Zehnder, E. C. Constable, *Liebigs Ann./Recueil* **1997**, 297.

[7] a) A. Tanatani, H. Kagechika, I. Azumaya, R. Fukutomi, Y. Ito, K. Yamaguchi, K. Shudo, *Tetrahedron Lett.* **1997**, *38*, 4425; b) R. Fukutomi, A. Tanatani, H. Kakuta, N. Tomioka, A. Itai, Y. Hashimoto, K. Shudo, H. Kagechika, *Tetrahedron Lett.* **1998**, *39*, 6475; c) A. Tanatani, K. Yamaguchi, I. Azumaya, R. Fukutomi, K. Shudo, H. Kagechika, *J. Am. Chem. Soc.* **1998**, *120*, 6433.

[8] K. P. Meurer, F. Vögtle, *Top. Curr. Chem.* **1985**, *127*, 1.

  0947-6539/01/0713-2808 $ 17.50+.50/0

[9] For representative examples, see: a) M. S. Newman, D. Lednicer, *J. Am. Chem. Soc.* **1956**, *78*, 4765; b) R. H. Martin, G. Morren, J. J. Schurter, *Tetrahedron Lett.* **1969**, *42*, 3684; c) R. H. Martin, N. Defay, H. P. Figeys, M. Flammang-Barbieux, J. P. Cosyn, M. Gelbcke, J. J. Schurter, *Tetrahedron* **1969**, *25*, 4985; d) T. W. Bell, H. Jousselin, *J. Am. Chem. Soc.* **1991**, *113*, 6283; e) C. Nuckolls, T. J. Katz, L. Castellanos, *J. Am. Chem. Soc.* **1996**, *118*, 3767; f) B. Kiupel, C. Niederalt, M. Nieger, S. Grimme, F. Vögtle, *Angew. Chem.* **1998**, *110*, 3206; *Angew. Chem. Int. Ed.* **1998**, *37*, 3031.

[10] a) Y. Dai, T. J. Katz, D. A. Nichols, *Angew. Chem.* **1996**, *108*, 2230; *Angew. Chem. Int. Ed. Engl.* **1996**, *35*, 2109; b) R. B. Prince, T. Okada, J. S. Moore, *Angew. Chem.* **1999**, *111*, 245; *Angew. Chem. Int. Ed.* **1999**, *38*, 233.

[11] J. C. Nelson, J. G. Saven, J. S. Moore, P. G. Wolynes, *Science* **1997**, *277*, 1793.

[12] a) C.-Y. Huang, V. Lynch, E. V. Anslyn, *Angew. Chem.* **1992**, *104*, 1259; *Angew. Chem. Int. Ed. Engl.* **1992**, *31*, 1244; b) S. J. Geib, C. Vicent, E. Fan, A. D. Hamilton, *Angew. Chem.* **1993**, *105*, 83; *Angew. Chem. Int. Ed. Engl.* **1993**, *32*, 119; c) I. L. Karle, D. Ranganathan, V. Haridas, *J. Am. Chem. Soc.* **1997**, *119*, 2777; d) N. Kimizuka, T. Kawasaki, K. Hirata, T. Kunitake, *J. Am. Chem. Soc.* **1995**, *117*, 6360.

[13] a) V. Berl, I. Huc, R. G. Khoury, M. J. Krische, J.-M. Lehn, *Nature* **2000**, *407*, 720; b) V. Berl, I. Huc, R. G. Khoury, J.-M. Lehn, *Chem. Eur. J.* **2001**, *7*, 2810, following paper in the present issue.

[14] V. Berl, M. J. Krische, I. Huc, J.-M. Lehn, M. Schmutz, *Chem. Eur. J.* **2000**, *6*, 1938.

[15] a) F. Mohamadi, N. G. Richards, W. C. Guida, R. Liskamp, M. Lipton, C. Caufield, G. Chang, T. Hendrickson, W. C. Still, *J. Comput. Chem.* **1990**, *11*, 440–467; b) S. J. Weiner, P. A. Kollman, D. Case, U. C. Singh, G. Alagona, S. Profeta, P. Weiner, *J. Am. Chem. Soc.* **1984**, *106*, 765.

[16] S. M. Redmore, C. E. F. Rickard, S. J. Webb, L. J. Wright, *Inorg. Chem.* **1997**, *36*, 4743.

[17] Y. H. Kim, J. Calabrese, C. McEwen, *J. Am. Chem. Soc.* **1996**, *118*, 1545.

[18] T. A. Halgren, *J. Comput. Chem.* **1996**, *17*, 490.

[19] F. Mohamadi, N. G. Richards, W. C. Guida, R. Liskamp, M. Lipton, C. Caufield, G. Chang, T. Hendrickson, W. C. Still, *J. Comput. Chem.* **1990**, *11*, 440.

[20] M. F. van Gunsteren, H. J. C. Berendsen, *Mol. Simul.* **1988**, *1*, 173.

[21] W. C. Still, A. Tempczyk, R. C. Hawley, T. Hendrickson, *J. Am. Chem. Soc.* **1990**, *112*, 6127.

[22] K. Motesharei, D. C. Myles, *J. Am. Chem. Soc.* **1998**, *120*, 7328.

[23] For a review of the use of Fmoc protection, see: E. Atherton, R. C. Sheppard, *The Fluorenylmethoxycarbonyl Amino Protecting Group*, in *The Peptides*, *Vol. 9* (Eds.: S. Udenfriend, J. Meierhofer), Academic Press, Orlando, Florida, **1987**, pp. 1–38.

[24] T. A. Kelly, D. W. McNeil, *Tetrahedron Lett.* **1994**, *35*, 9003.

[25] R. S. Lott, V. S. Chauhan, C. H. Stammer, *J. Chem. Soc. Chem. Commun.* **1979**, 495.

Received: January 8, 2001 [F2989]